Biophysical Chemistry 42 (1992) 79–85
Elsevier Science Publishers B.V., Amsterdam

BIOCHE 01614

Solvent effects on myoglobin conformational substates as studied by electron paramagnetic resonance

A.R. Bizzarri

ISAS - International School for Advanced Studies, Strada Costiera 11, I-34014 Trieste (Italy)

and

S. Cannistraro *

Gruppo di Biofisica Molecolare, Dipartimento di Fisica, Università di Perugia, I-06100 Perugia (Italy)

(Received 14 March 1991; accepted in revised form 6 June 1991)

Abstract

Electronic paramagnetic resonance spectra of frozen horse myoglobin solutions at two different pH values and with different added organic solvents are analyzed by computer simulation in terms of Gaussian distributions of some ferric ion crystal field parameters. The mean values and the corresponding variances of these distributions, thought as arising from a distribution of the protein conformational substates, are found to be affected by both the pH and the addition of organic solvents. The significant narrowing of the conformational substate distribution, induced by large addition of glycerol, is discussed.

Keywords: Myoglobin; Conformational substates; Electronic paramagnetic resonance; Molecular dynamics

1. Introduction

It is well ascertained that proteins exist in many nearly isoenergetic substates which are thermally accessible and are relevant to their biological functionality [1,2]. On cooling below 160–180 K the various molecules are frozen into different substates and transitions among these substates are practically absent [3]. The most significant experimental evidence for these conformational substates (CS) is provided by the CO rebinding kinetics studies performed on myoglobin (Mb) water–glycerol solutions [4]. Myoglobin molecules, assuming different conformational substates, encompass a wide range of structures which perform the same function but with different rates and which may be modulated by external agents such as pressure, pH and solvent [5–7].

Many other experimental investigations conducted by inelastic neutron scattering [8], X-ray diffraction [9] and Mössbauer spectroscopy [10] lend support to the existence of CS in Mb and in other biological macromolecules. Moreover, molecular dynamics simulations have shown that the energy surface of Mb is characterized by a

* To whom correspondence should be addressed.

0301-4622/92/$05.00 © 1992 – Elsevier Science Publishers B.V. All rights reserved

large number of thermally accessible minima [11]. Under some aspects biomolecules show a close similarity with glasses and spin-glasses [12,13]. Low temperature thermal and dielectric properties of proteins show low energy excitations similar to those found in glasses; their anomalies in the vibrational density of states having been described in the framework of the two level tunneling system (TLS) model [14–16].

Electronic paramagnetic resonance (EPR) spectra of some copper proteins and of some Cu^{2+}-doped glasses formed by water and a second component show that these systems are characterized by a distribution of ligand field strengths onto the metal ion; such a distribution having been put into relation with the distribution of the CS energies in both the metallo-proteins and the amorphous matrices [17,18]. In this context, it has been suggested that the glass-like state in proteins is coupled to a structural heterogeneity which could be due to randomized local arrangements of certain atoms or groups of atoms and that hydration water could play a crucial role in the dynamics of conformational transitions [19–21]. On the other hand, EPR spectroscopy entails the advantage that the samples to be analyzed should not be necessarily transparent as is required, on the contrary, by optical spectroscopies (optical experiments in refs. [3–5] are performed in the presence of glycerol). Such a consideration, together with experimental evidences that EPR spectroscopic features [22–24] are affected by some solvents, sometimes used to make a glass, led us to investigate more deeply the role of solvent on Mb conformational substates.

The modifications in the high spin Mb EPR spectra, observed at 77 K, induced by the presence of different organic solvents (methanol, ethanol and glycerol) and at two different pH values, have been analyzed in terms of a distribution of some relevant Fe^{3+} ion crystal field parameters. In particular, the distributions of the ratio, E/D, between the rhombic and the axial zero field splitting and of the spin orbit higher state mixing coefficient η have been extracted by a careful computer simulation and have been discussed in connection with the CS distribution as also put into evidence by optical spectroscopy.

2. Materials and EPR spectral analysis

Aqueous Mb EPR samples at two pH values were prepared by dissolving commercial lyophilized horse skeletal muscle Mb in buffers (Sigma Chem. Co.). The highest concentration of Mb in the solutions was about 5 m*M*. Ferricyanide was used to oxidize the heme iron to the ferric valence state and the solutions were dialyzed several times against buffers to remove the oxidant. Aliquots of concentrate methanol, ethanol and glycerol buffer solutions were added to Mb solutions until the required concentration was reached. All the chemicals used were of analytical reagent grade. EPR spectra were recorded at 77 K by an X-band Varian E109 spectrometer equipped with a variable temperature control. EPR data acquisition was carried out on an HP 86A personal computer through a home made interface connected to a IEEE 488 bus [25]. To run simulations and best-fit programs, the same microcomputer was switched to an intelligent terminal of the mainframe computer (VAX 8350), through a serial interface and an HP terminal emulator.

It is well-known that ferric met-Mb EPR spectrum below pH 7 is characterized by two resonances, one at $g \cong 6$ and another at $g \cong 2$ (spectrum not-shown). The weak ligand (H_3O^+) to the sixth coordinate position of iron, determines an high spin state, $S = \frac{5}{2}$, and the system can be described by the spin Hamiltonian

$$H_s = g_e \mu_B \boldsymbol{H} \cdot \boldsymbol{S} + D\left[S_z^2 - S(S+1)/3\right] + E\left(S_y^2 - S_x^2\right) \qquad (1)$$

where the first term is the Zeeman contribute and D and E are the axial and rhombic zero-field splittings, respectively. In this spin state the condition of large zero field splitting is satisfied, so that only transitions within the lowest Kramers doublet occur and a fictitious spin $S = \frac{1}{2}$ can be used to fully represent the spin hamiltonian of the system; the corresponding Zeeman interaction, with axially symmetry ($g_x = g_y = g_\perp$), being expressed by the Hamiltonian

$$H = g_\parallel \mu_B H_z S_z + g_\perp \mu_B \left(H_x S_x + H_y S_y\right) \qquad (2)$$

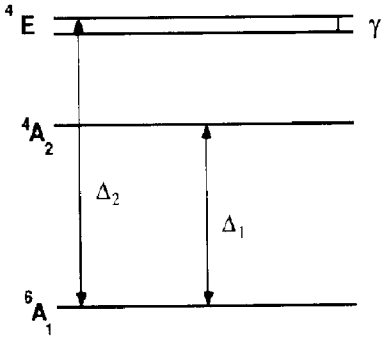

Fig. 1. Energy level diagram of the low-lying electronic states of high-spin heme. It has been assumed $\Delta_1 \approx 2000\ cm^{-1}$, $\Delta_2 \approx 6000\ cm^{-1}$, $\gamma \approx 60\ cm^{-1}$ [28].

The in-plane $g_\perp$ values for the ground doublet, including small high order corrections arising from spin orbit mixing of the excited quartet states into the lowest Kramers doublet, are given by [26–28]

$$g_{x,y} = 6.01 \pm 24E/D - 18.7(E/D)^2 - 12\eta^2 \quad (3)$$

where the ratio E/D is given by

$$\frac{E}{D} = \frac{1}{2}\frac{\gamma}{\Delta_2}\frac{\Delta_t}{(\Delta_2 - \Delta_1)} \quad (4)$$

and the spin-orbit mixing of excited quartet states into the lowest Kramers doublet η is

$$\eta^2 = \frac{\lambda^2}{5}\left(\frac{1}{\Delta_1^2} + \frac{1}{\Delta_2\Delta_t} + \frac{1}{\Delta_2^2}\right) \quad (5)$$

where λ is the effective spin-orbit coupling constant ($\lambda \sim 300\ cm^{-1}$), and Δ_1, Δ_2 and γ are the difference energies of the low-lying electronic states of high spin ferric heme (see Fig. 1).

In a general way, the derivative field-swept EPR absorption spectrum, related to randomly oriented paramagnetic centers with $S = \frac{1}{2}$, can be reproduced by an expression of the type

$$\frac{dS(H)}{dH} = \iint_0^{\frac{\pi}{2}} \frac{P(\theta,\phi)}{g(\theta,\phi)}\frac{df(H)}{dH}\sin\theta\, d\theta\, d\phi \quad (6)$$

where the $1/g$ Aasa–Vanngård correction has been included [29]. $P(\theta, \phi)$ is the orientation-dependent transition probability, which, for a system with $S = \frac{1}{2}$, can be exactly calculated [30] to be

$$P(\theta,\phi) = g_x^2 + g_y^2 + g_z^2 - \frac{1}{g^2(\theta,\phi)} \times \left[g_x^4 \sin^2\theta\cos^2\phi + g_y^4 \sin^2\theta\cos^2\phi + g_z^4\cos^2\theta\right] \quad (7)$$

Our experimental spectra have been fitted by means of expressions (6) and (7), and by using a Lorentzian lineshape for $f(H)$ with an half-width at half-height of 25 gauss. According to the Isomoto et al. algorithm [30], once g_x, g_y and g_z have been fixed, the resonance field H is calculated for each orientation (θ, ϕ) and the spectrum $dS(H)/dH$ is computer-generated by carrying on the integration in eq. (6) as a sum over θ (in steps of one degree) and over ϕ (in steps of three degrees).

According to previous papers [17,18,21], we assume that the presence of a frozen CS distribution entails a distribution of the crystal field parameters Δ_1, Δ_2 and γ; this results in a distribution of E/D and η [see eqs. (4) and (5)] which, in turn, affect g_x and g_y (see eq. 3). The departure of g_x and g_y from $g_\perp$ determines changes in the shape and in the width of the $g \cong 6$ line [31,32]. To take into account for such an effect in agreement with other authors [32–34], we introduce in the simulation model two independent Gaussian distributions for the crystal field parameters E/D and η. In such a way, the resulting simulated spectrum can be visualized as a superposition of different spectra associated to different couples $(E/D, \eta)$ and then to different g_x, g_y values. It should be noted that Δ_1, Δ_2 and γ distributions can be worked out from the corresponding E/D and η distributions through eqs. (4) and (5). An analysis directly based on the Δ_1 and Δ_2 crystal field parameters will be presented in a forthcoming paper.

Computer-synthesized spectra have been used to fit the experimental EPR spectra in order to determine the parameters $(E/D)_0$, $\sigma_{E/D}$, η_0, σ_η characterizing the two Gaussian distributions.

Practically, the χ^2-function

$$\chi^2 = \sum_{i=1}^{N} \left[\frac{I^{\exp}(H_i) - I^{\sin}(H_i, p)}{\sigma_i} \right]^2 \qquad (8)$$

has been minimized by a simulated annealing approach [35]. $I^{\exp}(H_i)$ is the derivative of the experimental EPR absorption spectrum sampled at 500 discrete points of the magnetic field, $I^{\sin}(H_i, p)$ is the simulated spectrum function that also depends on the parameter set $p((E/D)_0, \sigma_{E/D}, \eta_0, \sigma_\eta)$ and σ_i is the standard deviation calculated for the ith experimental point of the EPR spectrum by repeated runs.

3. Results and discussion

Figure 2 shows an example of the quality of the fits obtained by our simulation method. Actually, this figure shows an almost indistinguishable superposition between experimental and simulated EPR patterns. The experimental spectrum of pure Mb solutions, at pH = 6.7 (Fig. 2a), recorded at 77 K is shown only around its most significant region, i.e. around $g_\perp \cong 6$. The simulated spectrum provided a mean value, $(E/D)_0$, for the distribution related to the rhombicity, of 3.2×10^{-3} and a variance, $\sigma_{E/D}$, of 2.5×10^{-3}, while the mean value of the distribution related to the spin orbit mixing, η_0 and the variance, σ_η,

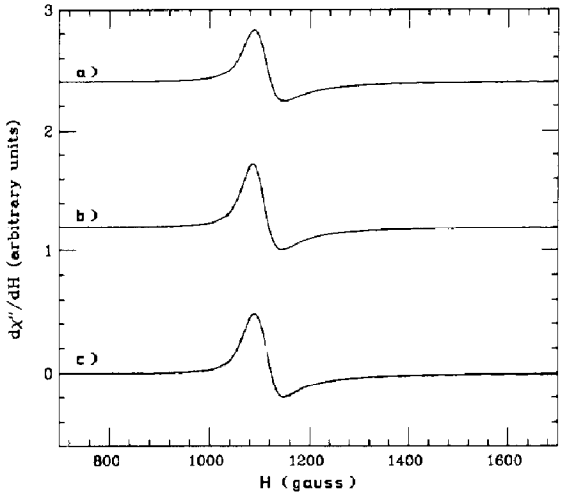

Fig. 2. Low-field X-band EPR spectra at 77 K of ferric Mb frozen solutions at pH = 6.7 of: (a) aqueous Mb solution; (b) aqueous Mb solution in presence of methanol (1:1 heme-to-alcohol molar concentration); (c) aqueous Mb solution in presence of glycerol (1:1 water/glycerol volume). The superimposed dashed lines show the related simulated EPR patterns.

were found to be 7.4×10^{-2} and 2.4×10^{-2} respectively (see Table 1). $(E/D)_0$ and η_0 values are in agreement with experimental values reported for a ferric-met-Mb single crystal [26]. Moreover $(E/D)_0$ and $\sigma_{E/D}$ values are in a good agreement with the results obtained by simulations by Brill et al. [33]; while η_0 and σ_η values differ quite significantly from the values reported by these authors.

Table 1

Crystal field parameter distributions obtained by simulation of the experimental EPR spectra of ferric Mb frozen solutions. The σ_g values are calculated from eq. (9). Mb concentration is 5×10^{-3} M, methanol and ethanol concentration is equal to that of heme, glycerol volume is in ratio 1:1 with water. The 68% confidence limits are included around changes of 40% for $(E/D)_0$, of 30% for $\sigma_{E/D}$, of 10% and 40% for η_0 and σ_η respectively.

Sample	$(E/D)_0$ ($\times 10^3$)	$\sigma_{E/D}$ ($\times 10^3$)	η_0 ($\times 10^2$)	σ_η ($\times 10^2$)	σ_g ($\times 10^2$)
Mb pH 5.6	2.7	4	7.5	2.5	10.6
Mb pH 6.7	3.2	2.5	7.4	2.4	7.3
Mb + Methanol pH 5.6	2.4	3.9	7.7	2.4	10.3
Mb + Methanol pH 6.7	2.8	2.1	7.8	2.4	6.7
Mb + Ethanol pH 5.6	3.8	3.3	7.6	2.1	8.8
Mb + Ethanol pH 6.7	3.8	2.4	8.1	1.4	6.3
Mb + Glycerol pH 5.6	3.6	1.9	7.6	1.9	5.7
Mb + Glycerol pH 6.7	4.0	1.6	8.0	1.1	4.4

At a visual inspection the agreement between experimental and fitted patterns in Fig. 2 appears very good, however the goodness of the fits has been confirmed by the χ^2-test: in all the simulations, the probability that χ^2 is greater than χ_0^2 (where χ_0^2 is the calculated value by taking into account for the degrees of freedom) is larger than 0.95.

The crystal field distribution parameters related to Mb solutions in the presence of different added solvents, at two different pH values, are reported in Table 1. Before going into details it should be remarked that modifications of the spectra, as resulting from addition of solvents and from pH changes, could be immediately observed in the peak to peak linewidth at $g \cong 6$ and in the ratio between the positive and the negative (with respect to the baseline) part of this EPR line.

If we now look at Table 1, we observe that a lowering of pH from 6.7 to 5.6 results, for almost all the samples investigated, in a decrease of the mean values of the E/D and η distributions (see columns 1 and 3). Exceptions are constituted by $(E/D)_0$ in the presence of ethanol and by η_0 for pure Mb solutions; these values being not appreciably affected by the pH. If we now compare the results among samples at the same pH value, we remark that addition of aliquots (up to 5×10^{-3} M; i.e. 1:1 heme to alcohol molar concentration) of methanol induces a decrease of $(E/D)_0$ and an increase of η_0; while addition of small quantities of ethanol (up to 5×10^{-3} M) and of large quantities (1:1 water/glycerol volume) of glycerol cause a significant increase in $(E/D)_0$ and η_0.

Therefore, addition of solvents and/or changing the pH can alter the mean values of the crystal field parameter distributions. In general, the effects of the crystal field parameters induced by the presence of methanol and ethanol, at a concentration nearly equal to that of heme, can be attributed to local changes of the crystal field around the metal ion; in fact it is known that these alcohols bind to the metal ion [36]. On the contrary, since small additions of glycerol (1:1 heme-to-glycerol molar concentration) lead to no change both in the lineshape and in the crystal field parameter distributions, modifications of these distributions caused by large addition of glycerol are to be attributed to changes in the protein solvent interaction [7,19,20].

More interesting informations could be drawn from columns 2 and 4 of Table 1, in which the variances $\sigma_{E/D}$ and σ_η of the E/D and η distributions, respectively, are presented. For what concerns the effect of pH on these parameters, we can see that, for all the studied samples, larger values for $\sigma_{E/D}$ and for σ_η correspond to the lower pH value; this being particularly evident for the E/D distribution.

Addition of methanol and ethanol generally causes small decreases of $\sigma_{E/D}$ and σ_η, while large addition of glycerol produces a remarkable lowering of both these variances. The most significant modifications are evident at pH = 6.7 at which reductions of 36% and of 54% are observed for $\sigma_{E/D}$ and σ_η, respectively, in presence of 50% of glycerol.

The observed effects on $\sigma_{E/D}$ and σ_η, as due to pH changes and to additions of solvents, can be taken into account by analyzing the σ_g values reported in the fifth column of Table 1. These values are obtained by the following relationship

$$(\sigma_g)^2 = (24 - 37.4(E/D)_0)^2 \sigma_{E/D}^2 + (24\eta_0)^2 \sigma_\eta^2 \qquad (9)$$

which has been derived from eq. (3) under the already-mentioned hypothesis of two independent Gaussian distributions for E/D and η. σ_g is then associated to the variances of the crystal field parameter distributions and can be assumed to be connected to the number of different crystal field arrangements [18,21]. In other words, we can suppose that to larger distribution widths ($\sigma_{E/D}$, σ_η) a larger number of systems with different crystal field structures corresponds. Then, σ_g can be seen as an empirical estimate of the heterogeneity of the system.

Methanol and ethanol addition produces a small decrease of σ_g which reflects a modification of the crystal field distribution involved by the local binding of alcohols the metal ion.

A lowering of pH causes an increase of σ_g both in the presence and in the absence of added organic solvents. Such a result seems to indicate

that a lowering of pH involves a broadening of the Mb CS distribution. Actually, effects of pH changes on the CS distribution have been observed by optical spectroscopy in MbCO–water–glycerol solutions [5], where modifications of the inhomogeneous broadening of the three infrared CO stretch bands (corresponding to different angles between the CO dipole and the heme normal) have been put into relation with changes in the CS distribution [37].

For what concerns glycerol, it is evident that its massive addition to Mb aqueous solution has a strong effect on σ_g. The most significant modification is observed at pH 5.6 where we have a reduction of σ_g higher than 40% passing from pure Mb solutions to Mb–glycerol solutions. As we have already pointed out, modifications of the crystal field distributions induced by glycerol can not simply attributed to local changes around the metal ion, rather it could be seen as a consequence of a global modification on the protein dynamics determining the CS landscape which is, in the end, frozen out [12,21]. This result underlines the importance of the role played by the solvent in the determination of the CS of the biomolecules. The presence of glycerol alters the water solvent properties and this may result in a change of the coupling between the protein and the solvent around it. In particular, the dynamics of formation and breaking of hydrogen bonds which provide a coupling mechanism between conformational substate transitions and water fluctuations [19] may be affected by glycerol. Moreover, glycerol addition involves an increase in the viscosity and a decrease of dielectric constant of the solvent; these changes could respectively lead to a damping of the protein motion and to a change in the shielding of the charged side groups [14,20]. Since, however, glycerol changes markedly the freezing temperature of the glass, solvent dependent effects on the CS population (like condensation or others) cannot be ruled out. To assess which one of these molecular mechanisms is operative would require a deeper investigation but, in any case, it should be remarked that modifications in the solvent properties can affect the CS distribution and this should be carefully taken into consideration in the analysis of the corresponding results from optical spectroscopy in which large amounts of glycerol are required to make the samples transparent.

Further informations about the role of solvent in protein dynamics might be obtained by submitting EPR Mb samples to different cooling histories; in fact it has been observed that the cooling rate can affect the thermodynamic behaviour of the adsorbed water in Mb and in other biomolecules [19]. Moreover, this kind of study could be also employed to extract informations about the CS energy distribution. In such a connection some preliminary results show that, while the EPR spectra of Mb are not affected in a significant way by the cooling history, on the contrary, EPR spectra related to hemoglobin solutions show a strong dependence on such a rate.

4. Conclusions

It should be pointed out that, owing to its high sensitivity in detecting microenvironmental fluctuations around the paramagnetic probes, EPR spectroscopy can be a promising tool to study the structural and dynamics properties of protein CS distribution and the related energy distribution. In particular, for Mb, our computer analysis has put into evidence a significant narrowing of the CS distribution caused by large addition of glycerol. This aspect has to be taken into consideration when the results obtained by optical spectroscopy in the presence of the same organic solvent are analyzed.

References

1 H. Frauenfelder, F. Parak and R.D. Young, Annu. Rev. Biophys. Biophys. Chem. 17 (1988) 451.
2 V.I. Goldanskii and Y.F. Krupyanskii, Quart. Rev. Biophys. 22 (1989) 39.
3 A. Ansari, J. Berendzen, D. Braunstein, B.R. Cowen, H. Frauenfelder, M.K. Hong, I.E.T. Iben, J.B. Johnson, P. Ormos, T.B. Sauke, R. Scholl, A. Schulte, P.J. Steinbach, J. Vittitow and R.D. Young, Biophys. Chem. 26 (1987) 337.
4 A. Ansari, J. Berendzen, S.F. Bowne, H. Frauenfelder, I.E.T. Iben, T.B. Sauke, E. Shyamsunder and R.D. Young, Proc. Natl. Acad. Sci. U.S.A. 82 (1985) 5000.

5 M.K. Hong, D. Braunstein, B.R. Cowen, H. Frauenfelder, I.E.T. Iben, J.R. Mourant, P. Ormos, R. Scholl, A. Schulte, P.J. Steinbach, A.H. Xie and R.D. Young, Biophys. J. 58 (1990) 429.
6 H. Frauenfelder, N.A. Alberding, A. Ansari, D. Braunstein, B.R. Cowen, M.K. Hong, I.E.T. Iben, J.B. Johnson, S. Luck, M.C. Marden, J.R. Mourant, P. Ormos, L. Reinisch, R. Scholl, A. Schulte, E. Shyamsunder, L.B. Sorensen, P.J. Steinbach, A.H. Xie, R.D. Young and K.T. Yue, J. Phys. Chem. 94 (1990) 1024.
7 L. Cordone, A. Cupane and S. Fornili, Biopolymers 22 (1983) 1677.
8 W. Doster, S. Cusack and W. Petry, Nature 337 (1989) 754.
9 H. Frauenfelder, G.A. Petsko and D. Tsernoglou, Nature 280 (1979) 558.
10 F. Parak and E.W. Knapp Proc. Natl. Acad. Sci. U.S.A. 81 (1984) 7088.
11 R. Elber and M. Karplus, Science 235 (1987) 318.
12 I.E.T. Iben, D. Braunstein, W. Doster, H. Frauenfelder, M.K. Hong, J.B. Johnson, S. Luch, P. Ormos, A. Schulte, P.J. Steinbach, A.H. Xie and R.D. Young, Phys. Rev. Lett. 62 (1989) 1916.
13 D.L. Stein, PNAS 82 (1985) 3670.
14 G.P. Singh, H.J. Schink, H.V. Lohneysen, F. Parak and S. Hunklinger, Z. Phys. B 55 (1984) 23.
15 I.S. Yang and A.C. Anderson, Phys. Rev. B34 (1986) 2942.
16 W.A. Philips, in: Amorphous Solids Low Temperature Properties, ed. W.A. Philips (Springer Verlag, Berlin, 1981) vol. 24.
17 S. Cannistraro, G. Giugliarelli, P. Marzola and F. Sacchetti, Solid State Commun. 68 (1988) 369.
18 S. Cannistraro, J. Phys. France 51 (1990) 131.
19 W. Doster, A. Bachleitner, R. Dunau, M. Hiebl and E. Luscher, Biophys. J. 50 (1986) 213.
20 G.P. Singh, F. Parak, S. Hunklinger and K. Dransfert, Phys. Rev. Lett. 47 (1981) 685.
21 M. Bacci and S. Cannistraro, Appl. Magn. Res. 1 (1990) 369.
22 D.O. Hearshen, W.R. Hagen, R.H. Sands, H.J. Grande, H.L. Crespi, I.C. Gunsalus and W.R. Dunham, J. Magn. Resonance 69 (1986) 440.
23 A.S. Brill, B.W. Castleman and M.E. McKnight, Biochemistry 15 (1976) 2309.
24 S. Cannistraro, Chem. Phys. Lett. 122 (1985) 165.
25 G. Giugliarelli, P. Tancini and S. Cannistraro, J. Phys. E (Sci. Instrum.) 22 (1989) 702.
26 M. Kotani Adv. Quantum Chem. 4 (1968) 227.
27 C.P. Scholes J. Chem. Phys. 52 (1970) 4890.
28 F.G. Fiamingo, A.S. Brill, D.A. Hampton and R. Thorkildsen Biophys. J. 55 (1989) 67.
29 R. Aasa and T. Vanngård, J. Magn. Resonance 19 (1975) 308.
30 A. Isomoto, H. Watari and M. Kotani, J. Phys. Soc. Jpn 29 (1970) 1571.
31 W. Blumberg and J. Peisach, Probes of structure and function of macromolecules and membranes (Academic Press, New York, NY, 1971).
32 S. Cannistraro, Studia Biophysica 98 (1983) 133.
33 A.S. Brill, F.G. Fiamingo and D.A. Hampton, J. Inorg. Biochem. 28 (1986) 137.
34 A.S. Yang and B.J. Gaffney, Biophys. J. 51 (1987) 55.
35 S. Kirkpatrick, C.D. Gelatt and M.P. Vecchi, Science 220 (1983) 671.
36 D.L. Ollis, P.E. Wright, J.M. Pope and C.A. Appleby, Biochemistry 20 (1981) 587.
37 P. Ormos, D. Braunstein, H. Frauenfelder, M.K. Hong, S.L. Lin, T.B. Sauke and R.D. Young, Proc. Natl. Acad. Sci. U.S.A. 85 (1988) 8492.